JACS
JOURNAL OF THE AMERICAN CHEMICAL SOCIETY
Article
pubs.acs.org/JACS

Details of the Ultrafast DNA Photo-Cross-Linking Reaction of 3-Cyanovinylcarbazole Nucleoside: *Cis*−*Trans* Isomeric Effect and the Application for SNP-Based Genotyping

Kenzo Fujimoto,*[,†,‡] Asuka Yamada,[†] Yoshinaga Yoshimura,[†] Tadashi Tsukaguchi,[§] and Takashi Sakamoto[†]

[†]School of Materials Science and [‡]Research Center for Bio-Architecture, Japan Advanced Institute of Science and Technology, 1-1 Asahi-dai, Nomi, Ishikawa 923-1292, Japan

[§]Faculty of Bioresources and Environmental Sciences, Ishikawa Prefectural University, 1-308 Suematsu, Nonoichi, Ishikawa 921-8836, Japan

Supporting Information

ABSTRACT: To clarify the *cis*−*trans* isomeric effect on the ultrafast DNA photo-cross-linking reaction of 3-cyanovinylcarbazole nucleoside (^{CNV}K) in the DNA duplex, which gives a single photodimer on the reversed-phase HPLC chromatogram, the kinetics of the *cis*−*trans* photoisomerization of ^{CNV}K in double-stranded DNA was evaluated. Since the photoisomerization rate constant for *cis* to *trans* isomerization in double-stranded DNA was significantly larger than that for *trans* to *cis* isomerization, and the thermodynamic stability of the *trans* isomer was higher than that of the *cis* isomer, it was strongly suggested that the *trans* isomer of ^{CNV}K is a reactive species of the photo-cross-linking reaction. ^{1}H−^{1}H NOESY analysis of the photoadduct consisting of ^{CNV}K and T also supported the *trans*-mediated photo-cross-linking reaction of ^{CNV}K. By using this ultrafast photo-cross-linking reaction for the molecular beacon-based SNPs typing, four individual Japanese rice strains were clearly distinguishable with simple photoirradiation and fluorescence imaging using double-stranded target DNAs.

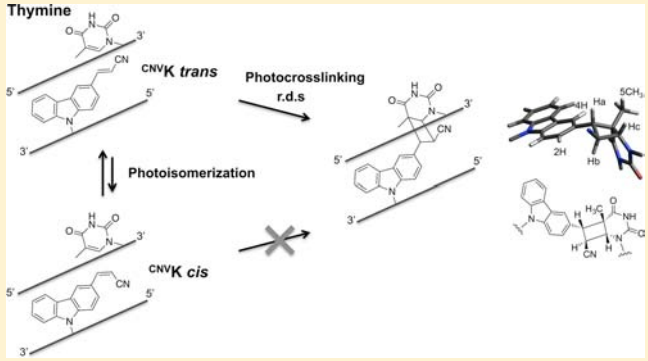

INTRODUCTION

DNA photo-cross-linking technology is an attractive tool for the detection, regulation, and manipulation of DNA and RNA. The sequence-specific and photoresponsive cross-linking manner enables us to detect, regulate, and manipulate the function and structure of target DNA and RNA at a desired timing with simple photoirradiation. For many years, psoralen and its related derivatives have been used as the photoreactive moiety to the pyrimidine base in target DNA or RNA strand. As the photoreactive oligonucleotides containing psoralen derivative stabilize DNA−DNA, DNA−RNA, and RNA−RNA duplex with the covalent bond formation,[1−5] the oligonucleotide is useful as a photoreactive antisense oligonucleotide,[6−8] a photoreactive antigene oligonucleotide,[9] and as a thermal stable staple oligonucleotide for DNA origami construction.[10]

In 2008, as the other class of photoreactive moiety for DNA photo-cross-linking, we successfully developed an artificial nucleoside that has a 3-cyanovinylcarbazole moiety instead of nucleobase (^{CNV}K).[11−14] The oligodeoxyribonucleotide-containing ^{CNV}K can photo-cross-link to a pyrimidine base at the −1 position in complementary DNA or RNA within a few seconds of photoirradiation.[15−17] This quick photo-cross-linking reaction is applicable for antisense strategy,[18] selection of miRNAs,[15] and construction and/or stabilization of nanostructured DNA.[19−21] Thus, we believe that ^{CNV}K has tremendous potential for biological and nanotechnological applications; however, details of the photo-cross-linking reaction, such as the *cis*−*trans* isomeric effect of the cyanovinyl group on ^{CNV}K, are still unclear. In the previous study, HPLC analysis after the photo-cross-linking reaction gave a single peak having the molecular mass of an oligonucleotide photodimer, suggesting strongly that the reaction occurred through either one of the *cis* or *trans* isomers of ^{CNV}K.[11]

In this study, the *cis*-*trans* isomeric effect on the photo-cross-linking reaction of ^{CNV}K in double-stranded DNA (dsDNA) was evaluated from the viewpoint of kinetics and the structure of the photo-cross-linking product. In addition, the applicability of the photo-cross-linking reaction for single nucleotide polymorphisms (SNP(s)) analysis using a photoreactive molecular beacon containing ^{CNV}K was evaluated.

Received: July 8, 2013
Published: October 2, 2013

dx.doi.org/10.1021/ja406965f | J. Am. Chem. Soc. 2013, 135, 16161−16167

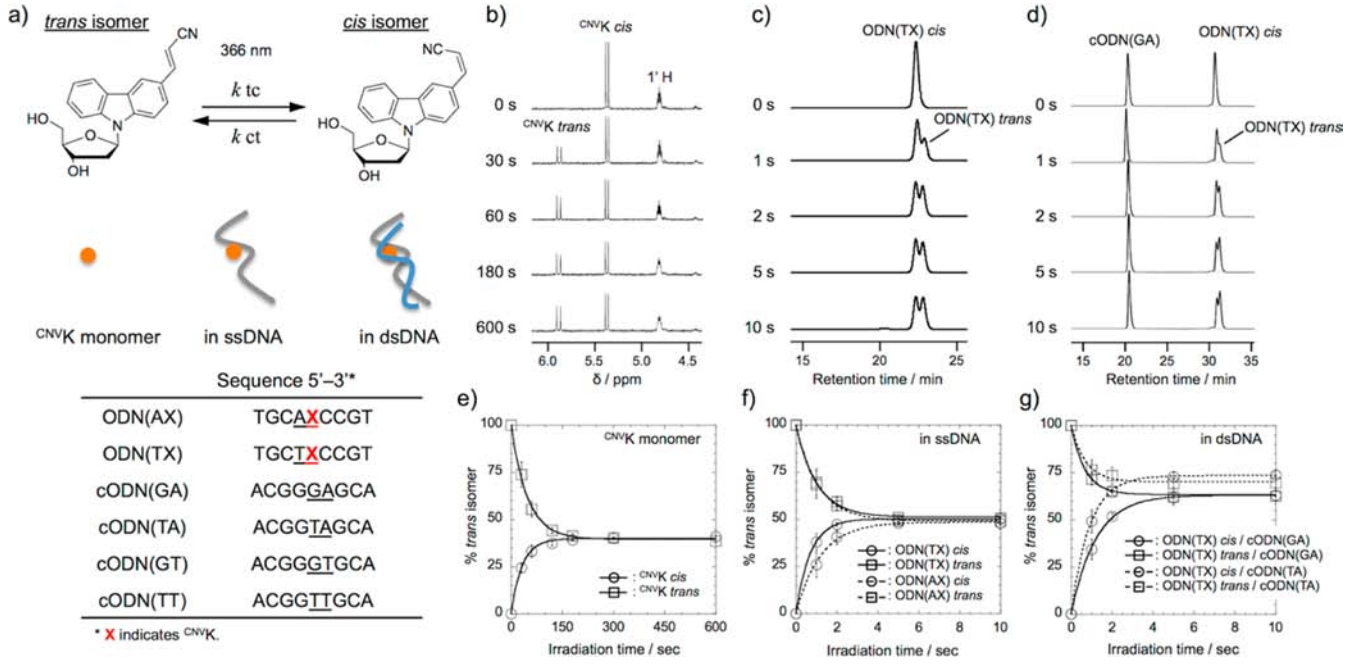

Figure 1. Photoisomerization of ^{CNV}K in monomer, ssDNA, and dsDNA. (a) Schematic drawing of the photoisomerization of ^{CNV}K and the sequences of oligonucleotides. (b) ^{1}H NMR spectra of isolated ^{CNV}K *cis* monomer in $CDCl_3$ after the left indicated time period of 366 nm photoirradiation and (e) the time course of the photoisomerization of isolated ^{CNV}K *cis* (○) and *trans* (□) monomer. (c) Reversed-phase HPLC chromatograms of isolated ODN(TX) *cis* in aqueous buffer solution (50 mM sodium cacodylate buffer (pH 7.4) containing 100 mM NaCl) after the indicated time period of 366 nm photoirradiation and (f) the time course of the photoisomerization of isolated ^{CNV}K *cis* (○) and *trans* (□) in ssDNA. (d) Reversed-phase HPLC chromatograms of the duplex consisting of isolated ODN(TX) *cis* and cODN(GA) in aqueous buffer solution after the indicated time period of 366 nm photoirradiation and (g) the time course of the photoisomerization of isolated ^{CNV}K *cis* (○) and *trans* (□) in dsDNA. All experiments were performed at 0 °C. Error bars indicate the standard deviations (n = 3).

MATERIALS AND METHODS

Oligonucleotide Synthesis and Preparation. All oligonucleotides having ^{CNV}K were synthesized by a 3400 DNA synthesizer (Applied Biosystems) and purified by a reversed-phase HPLC (JASCO PU-980, HG-980-31, DG-980-50, UV-970 system equipped with an InertSustain C18 column (GL Science, 5 μm, 10 × 150 mm)). Preparation of oligonucleotides was confirmed by MALDI-TOF-MS (see the Supporting Information Table S1). Phosphoramidite of ^{CNV}K was synthesized according to a method described in the literature.[11] Other oligonucleotides were purchased from Fasmac (Japan) and used without farther purification.

Kinetic Analysis of the Photoisomerization and Photo-Cross-Linking. ^{CNV}K monomer, single-stranded DNA (ssDNA) or dsDNA containing ^{CNV}K was irradiated by a transilluminator (366 nm, Funakoshi) and analyzed by ^{1}H NMR spectroscopy or reversed-phase HPLC.

Thermodynamic and Kinetic Analysis of the Hybridization. Melting temperatures of the duplexes were measured by a UV−vis spectrophotometer (JASCO, V-630bio) at 260 nm. The hybridization kinetics were measured by a surface plasmon resonance biosensor (GE, BIAcore J) with avidine chips that have biotine-modified cODNs on the surface. After the injection of various concentrations of ODNs the sensorgrams were collected.

^{1}H–^{1}H NOESY Measurement of the Photoadduct Consisting of ^{CNV}K and T. ODN(AX) (2 μmol) and cODN(GT) (2 μmol) were photo-cross-linked and digested with P1 nuclease and snake venom phosphodiesterase following alkaline phosphatase treatment. The photoadduct consisting of ^{CNV}K and T was purified by HPLC and subjected to NOESY experiments. ^{1}H–^{1}H NOESY was performed in CD_3CN with the Avance III NMR system (Bruker) at 25 °C. The mixing time is 650 ms.

Fluorescence Measurement and Imaging. Fluorescence spectra were measured by a spectrofluorometer (JASCO, FP-6500) with a 520 nm excitation. Measurements were performed using a microquartz crystal cell (optical path length; 2 mm) with 50 μL sample solution at 5 °C. Fluorescence images were recorded by a fluorescence imaging system (Fujifilm, LAS-3000) equipped with a 520 nm LED lamp. Samples (50 μL, [pMB] = [dsDNA] = 3 μM in 50 mM sodium cacodylate buffer (pH 7.4) containing 100 mM NaCl) were irradiated (366 nm, 1600 mW/cm^2, 1 min, 60 °C) and then imaged in plastic tubes (0.5 mL).

RESULTS AND DISCUSSION

Kinetics of the *Cis*–*Trans* Photoisomerization of ^{CNV}K in Monomer, ssDNA, and dsDNA. The *cis*–*trans* isomers of ^{CNV}K can clearly be distinguished on 1H NMR spectrum; 5.9 ppm (J = 17 Hz, *trans*), 5.4 ppm (J = 12 Hz, *cis*). Thus, at first, we performed NMR measurement of isomeric pure ^{CNV}K *cis* after the different time period of photoirradiation (Figure 1b). The original doublet signal at 5.4 ppm was decreased and a new doublet signal at 5.9 ppm appeared and increased with the photoirradiation, indicating that the photoisomerization had occurred and ^{CNV}K *trans* was generated by 366 nm photoirradiation. The time course of the photoisomerization (Figure 1e) suggests that the photoisomerization reaction reached the photoequilibrium state within ca. 200 s of photoirradiation. In the case of ^{CNV}K in ssDNA and dsDNA, the photoisomerization was analyzed by reversed-phase HPLC (Figure 1c and 1d). The two peaks on the HPLC chromatogram were purified and identified by a comparison between the ^{CNV}K from the enzyme-digested product of ODN and isomeric pure ^{CNV}K monomer on HPLC. As shown in Figure 1c,d, both in the case of ssDNA and dsDNA, the peak identical to ODN having ^{CNV}K *cis* was decreased and a new peak identical to ODN having ^{CNV}K *trans* was increased with the photoirradiation, indicating that the photoisomerization had occurred and ^{CNV}K *trans* was generated in ssDNA and dsDNA by 366 nm photoirradiation,

dx.doi.org/10.1021/ja406965f | J. Am. Chem. Soc. 2013, 135, 16161−16167

the same as with the ^{CNV}K monomer. The time course of the photoisomerization (Figure 1f,g) suggests that the photoisomerization reaction reached the photoequilibrium state within ca. 5 s of photoirradiation, both in the case of ssDNA and dsDNA. The kinetic parameters of the photoisomerization of ^{CNV}K in monomer, ssDNA and dsDNA were estimated from the time course shown in Figure 1e−g with the assumption of the first-order kinetics and the kinetic parameters of the photoisomerization are listed in Table 1. The photoisomerization rate constant of ^{CNV}K in dsDNA was larger than that in ssDNA. And the photoisomerization rate constant of ^{CNV}K in ssDNA was larger than that in monomer, suggesting that the stacking interaction around the ^{CNV}K largely affected the photoisomerization reaction. There is a tendency to increase the photoisomerization rate constant and the population of the *trans* isomer in the photoequilibrium state with the increase of the stacking interaction around the ^{CNV}K, suggesting that the *trans* isomer is favorable in dsDNA. The population of the *trans* isomer in ODN(TX)/cODN(TA) duplex at the photoequilibrium state was larger than that in the case of ODN(TX)/cODN(GA) duplex (Figure 1g), suggesting that the nucleobase possessed by the opposite site of ^{CNV}K also affected the *trans* favorability of ^{CNV}K in dsDNA.

Table 1. Photoisomerization Rate Constants of ^{CNV}K in ssDNA and dsDNA

	photoisomerization rate constant/s^{-1}[a]		
	k_{ct}	k_{tc}	k_{ct}/k_{tc}
monomer	0.007	0.013	0.54
In ssDNA			
ODN(AX)	0.400	0.413	0.97
ODN(TX)	0.408	0.486	0.84
In dsDNA			
ODN(TX)/cODN(GA)	0.573	0.493	1.16
ODN(TX)/cODN(TA)	0.870	0.384	2.27

[a]The values were estimated from the time courses shown in Figure 1e−g.

Kinetics of the Photo-Cross-Linking Reaction. To evaluate the *cis*−*trans* isomeric effect on the photo-cross-linking reaction, UPLC analysis of the dsDNA after the various time periods of 366 nm photoirradiation was performed (Figure 2a,b). In both cases, original strands were decreased and two new peaks having a molecular mass of photo-cross-linked dimer (5546.76 calcd for $[(M + H)^+]$, found 5546.63 (*cis*-ODN(AX)/cODN(GT)) and 5546.62 (*cis*-ODN(AX)/cODN(GT))) and *cis*−*trans* photoisomerized ODN(AX) appeared, indicating that the photo-cross-linking reaction had occurred without side reaction in both cases of *cis*-*trans* isomer. The observed rate constants (k_{obs}) for the photo-cross-linking reaction are shown in Table 2. In all cases, the values of k_{obs} were 3- to 5-fold smaller than that of the photoisomerization rate constant in dsDNA as shown in Table 1, suggesting that the photo-cross-linking reaction is a rate-determining step of the photo-cross-linking reaction. As in the case of the T possessed on the opposite site of ^{CNV}K, the photoisomerization rate constant of the *cis* to *trans* isomerization (Table 1), relatively large k_{obs} observed in the case of ODN(AX)/cODN(TT) duplex can be explained with the assumption that the *trans* isomer is the reactive species of the photo-cross-linking reaction.

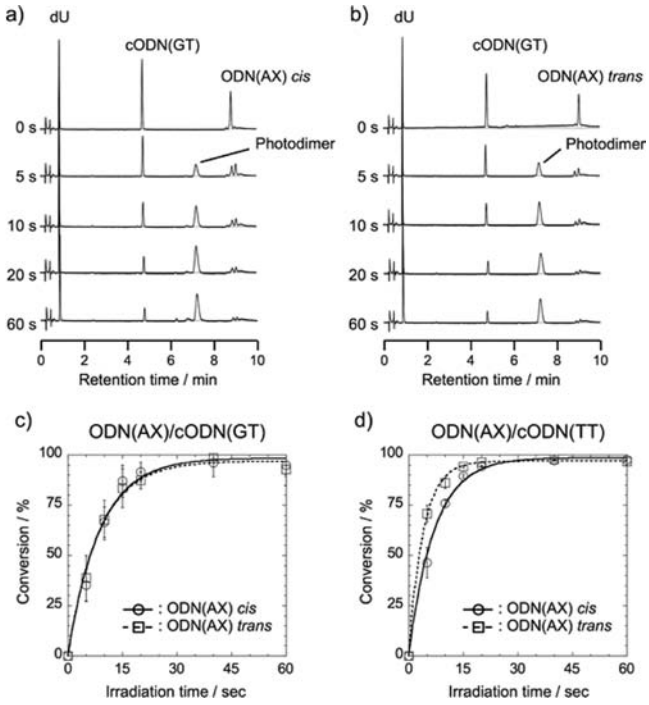

Figure 2. Photo-cross-linking reaction of ^{CNV}K *trans* and ^{CNV}K *cis* in dsDNA. UPLC chromatograms of the duplex consisting of ODN(AX) and cODN(GT) having isomeric pure (a) ^{CNV}K *cis* or (b) ^{CNV}K *trans* after the indicated time period of 366 nm photoirradiation and the time course of the photo-cross-linking reaction of isolated ODN(AX) *cis* or *trans* with (c) cODN(GT) and with (d) cODN(TT). The results of UPLC analysis of the duplex consisting of ODN(AX) and cODN(TT) are shown in Figures S4 (Supporting Information). [duplex] = 2 μM in 50 mM sodium cacodylate buffer (pH 7.4) containing 100 mM NaCl. All experiments were performed at 0 °C. Error bars indicate the standard deviations (n = 3).

Table 2. Observed Photo-Cross-Linking Rate Constants (k_{obs}) of Each Isomer of ^{CNV}K in dsDNA

	$k_{obs} \times 10^3$[a] (s^{-1})		
	trans	*cis*	*trans*/*cis*
ODN(AX)/cODN(GT)	117 ± 7	114 ± 11	1.03
ODN(AX)/cODN(TT)	250 ± 11	142 ± 7	1.76

[a]These values were estimated from the time course of the photo-cross-linking reaction (Figure 2c and d) with the assumption of first-order reaction kinetics.

Thermal Stability and Hybridization Kinetics of the Duplexes Containing ^{CNV}K. The thermal stability of the duplexes containing ^{CNV}K *trans* or *cis* was evaluated by UV melting experiments (Table 3 and Figure S5, Supporting Information). The melting temperatures (T_M(s)) of the duplexes were significantly dependent on the isomers of ^{CNV}K, and the duplexes containing *trans* isomer were more stable compared with *cis* isomer. These facts may contribute to the higher reaction rate of *cis* to *trans* photoisomerization in dsDNA observed in the photoisomerization kinetics experiment described above. The hybridization kinet ics of the duplexes containing *trans* or *cis* isomer was also evaluated by SPR experiments (Table 3 and Figure S6, Supporting Information). The association rate constant (k_a) of ODNs having ^{CNV}K *trans* were 2 to 3−fold larger than that of ODNs having ^{CNV}K *cis*,

dx.doi.org/10.1021/ja406965f | J. Am. Chem. Soc. 2013, 135, 16161−16167

Table 3. Hybridization Profiles of ODN Containing ^{CNV}K *Trans* or *Cis*

		T_M[a] (°C)	$k_a \times 10^{4}$[b] (M^{-1} s^{-1})	k_d[b] (s^{-1})	$K_D \times 10^{6}$[b] (M)
ODN(AX)/cODN(GT)	*trans*	39.8 ± 0.4	5.58 ± 1.01	0.16 ± 0.03	2.89
	cis	35.6 ± 0.2	1.62 ± 0.70	0.15 ± 0.07	9.43
ODN(AX)/cODN(TT)	*trans*	37.9 ± 0.7	2.30 ± 0.64	0.11 ± 0.03	4.72
	cis	28.4 ± 2.2	1.20 ± 0.50	0.12 ± 0.05	10.0

[a] T_Ms were estimated from the UV melting curves (Figure S5, Supporting Information). [b] Kinetic parameters of the hybridization were estimated from SPR experiments (Figure S6, Supporting Information).

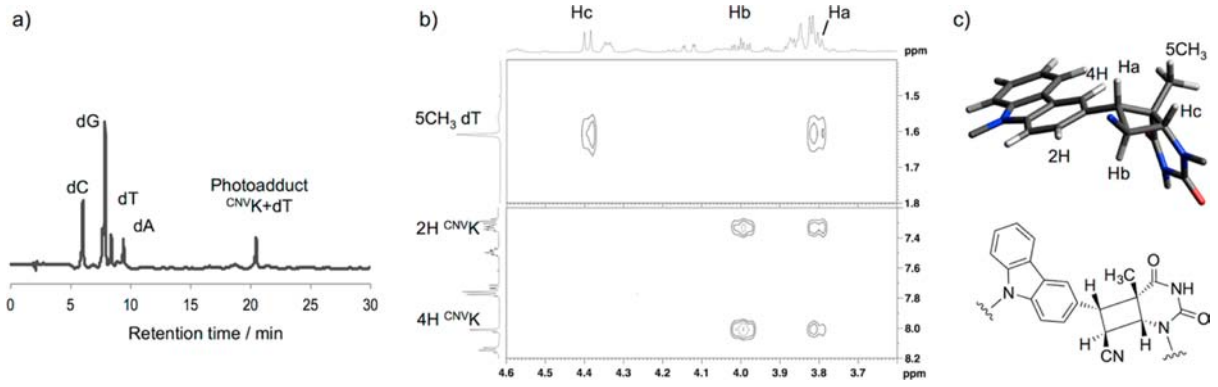

Figure 3. (a) Reversed-phase HPCL chromatogram of the product after the nuclease and phosphatase treatment of photodimer consisting of ODN(AX) and cODN(GT). (b) 2D ^{1}H–^{1}H NOESY spectrum of the photoadduct consisting of ^{CNV}K and T. Mixing time: 650 ms. (c) Determined structure of the photoadduct consisting of ^{CNV}K and T.

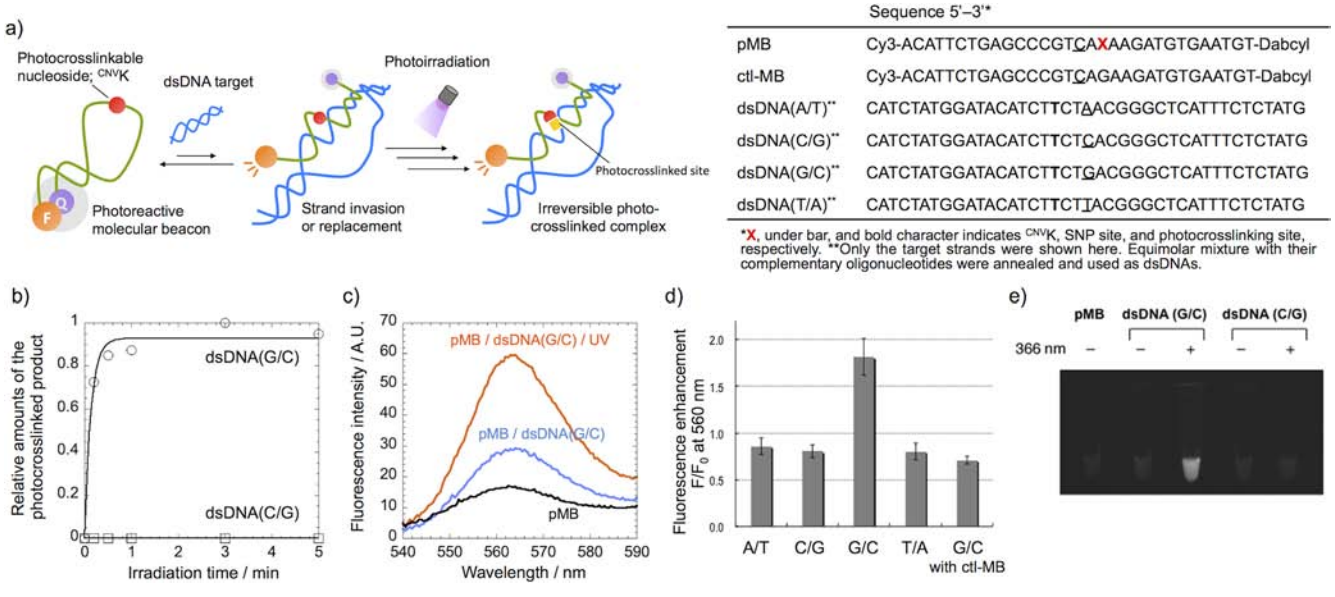

Figure 4. Fluorescence detection of target allele in double-stranded DNA using pMB. (a) Schematic drawing of allele specific photo-cross-linking reaction of pMB toward dsDNA target. (b) Time course of the photo-cross-linking reaction between pMB and dsDNAs. Mixture of pMB and dsDNA (30 μL, [pMB] = 3 μM, [dsDNA] = 1 μM in 50 mM sodium cacodylate buffer (pH 7.4) containing 100 mM NaCl) was irradiated at 60 °C and then subjected to PAGE analysis (Figure S9, Supporting Information). (c) Fluorescence spectra of pMB before and after the photoirradiation. [pMB] = [dsDNA] = 5 nM in 50 mM sodium cacodylate buffer (pH 7.4) containing 20 mM $MgCl_2$. Photoirradiation was performed at 60 °C for 10 s. Fluorescence spectra were measured at 5 °C with excitation at 520 nm. (d) Fluorescence enhancement of the pMB in the presence of various target dsDNAs. Conditions were the same as those in panel c. (e) Fluorescence image of the pMB in the presence of dsDNA target. [pMB] = [dsDNA] = 3 μM in 50 mM sodium cacodylate buffer (pH 7.4) containing 100 mM NaCl. After the photoirradiation (1 min, 60 °C), fluorescence imaging was performed with the image analyzer.

suggesting that the *trans* isomer has a more favorable structure for hybridization in the single-stranded state.

Structure of the Photoadduct Consisting of ^{CNV}K and T. As shown in Figure 3a, in the HPLC chromatogram of the product after the enzymatic digestion of photodimer consisting of ODN(AX) and cODN(GT), only one peak that has the molecular mass identical to the photodimer consisting of ^{CNV}K and T (577.22, calcd for [(M + H)$^+$], found 577.59) appeared after the photoirradiation, strongly suggesting that the photo-cross-linking reaction had occurred through either one of the *cis* or *trans* isomers of ^{CNV}K. To identify the reactive isomer of the photo-cross-linking reaction, we performed structural analysis

dx.doi.org/10.1021/ja406965f | J. Am. Chem. Soc. 2013, 135, 16161–16167

of the photoadduct consisting of ^{CNV}K and T by NMR experiments. The signals of 3 protons on the cyclobutane ring (Ha, Hb, and Hc in Figure 3c) were assigned by ^{1}H−^{1}H COSY, ^{1}H−^{13}C HSQC, ^{1}H−^{13}C HMBC (Figure S7, Supporting Information) and ^{1}H−^{1}H NOESY experiments (Figure 3b). In ^{1}H−^{13}C HMBC experiment, three cross peaks with C5 methyl proton of thymidine, 50, 52, and 170 ppm, were detected (Figure S7, Supporting Information), suggesting that these carbons possess 3 bonds distance from the C5 methyl proton. As the signal at 170 ppm can be assigned as C4 carbon of thymidine, we assigned signals at 50 and 52 ppm as the carbons attached with Ha or Hc. As the signal at 50 and 52 ppm has the cross peak with 3.8 and 4.4 ppm in ^{1}H−^{13}C HSQC spectrum (Figure S7, Supporting Information), protons having the signal at 3.8 and 4.4 ppm can be assigned as Ha or Hc. Together with ^{1}H−^{1}H NOESY experiment as shown in Figure 3b; i.e., the proton at 3.8 ppm has cross peaks with phenyl proton (2H and 4H) on carbazole ring and the proton at 4.4 ppm did not; we successfully assigned the protons on cyclobutane ring as shown in Figure 3b,c. In the ^{1}H−^{1}H NOESY spectrum (Figure 3b and Figure S8, Supporting Information), there was a strong NOE signal of Ha and Hc with 5CH_3 of the thymine base, although the NOE signal of Hb with 5CH_3 was not observed, indicating that the distance between Ha or Hc and 5CH_3 is closer than that between Hb and 5CH_3. In addition, the strong NOE signals of Ha and Hb with protons at the 2 and 4 position of the carbazole ring, and Ha with Hc, and weak NOE signals of Hb with Ha or Hc were observed, suggesting strongly that the *trans* isomer of ^{CNV}K reacted with the thymine base and formed a cyclobutane ring having the geometry as shown in Figure 3c. The coupling constant of Hc with Hb (8.1 Hz) was consistent with the reported coupling constant of H6−H6 in the case of *trans-syn* T−T photodimer,[22,23] suggesting that the Hc and Hb of the photodimer consisting of ^{CNV}K and T has the same geometry as H6−H6 of *trans-syn* T-T dimer. This result also supports the geometry of the cyclobutane ring as shown in Figure 3c.

Photoreactive Molecular Beacon for Genotyping Using dsDNA Target. A molecular beacon (MB) is a powerful tool for detecting nucleic acids, such as RNA imaging in cells[24−26] and typing of single nucleotide polymorphisms (SNP(s)) using the ssDNA target.[27−30] However, it is difficult to obtain the MB targeting dsDNAs because of the high stability of the dsDNA target. A peptide nucleic acid (PNA) based MB, which has the strand invasion activity, is the only solution reported to date.[31,32] Although the PNA-based method is superior, there are some disadvantages such as its low solubility[33] and high binding affinity to mismatch sequence. Therefore, an alternative method that can selectively detect the target sequence in dsDNA is required. The photo-cross-linking reaction of ^{CNV}K provides a solution to this problem, that is, the photo-cross-linking between MB and the target strand in dsDNA is expected to stabilize the double strand with the formation of an irreversible photo-cross-linked complex, and the strand displacement or invasion would be accelerated, so that the sequence specific SNPs detection of the dsDNA target becomes possible. To demonstrate this concept (Figure 4a), ^{CNV}K was incorporated into the loop region of MB for the SNP site from the rice genome, and the feasibility of the photoreactive MBs (pMB(s)) for SNPs analysis was evaluated. As a fluorescent dye and quencher, Cy3 and Dabcyl were adopted. The sequences of the pMB and the target dsDNAs are shown in Figure 4. First, we evaluated the allele selectivity of the photo-cross-linking reaction between pMB and dsDNAs by denaturing PAGE analysis (Figure S9, Supporting Information, and 4b). Only in the case of dsDNA (G/C), which has a complementary sequence for the loop region of the pMB, a shifted band having low mobility appeared by 366 nm irradiation (Figure S9, Supporting Information, lane 6), indicating that the photo-cross-linking reaction occurred in a target allele specific manner. In all cases, 366 nm irradiation also caused the production of a higher mobility band, indicating that the unexpected intramolecular photo-cross-linking reaction had occurred. The photo-cross-linking reaction reached a plateau with 30 s irradiation (Figure 4b), indicating that the photo-cross-linking reaction was sufficiently fast, although the rate was approximately 20−fold slower than that in the case of the photo-cross-linking between an unstructured oligonucleotide containing the ^{CNV}K and ssDNA target. This delay of the reaction suggested the occurrence of the equilibrium shift toward a pMB/dsDNA-complexed state by the photoirradiation. These results suggest that the pMB specifically photo-cross-linked to the target DNA strand in dsDNA having the target allele via strand invasion or replacement process. After 366 nm irradiation, the fluorescence spectrum of the pMB in the presence of dsDNA (G/C) was measured by a spectrofluorophotometer (Figure 4c). The fluorescence intensity of pMB was 2-fold enhanced by the photoirradiation, indicating that the allele specific photo-cross-linking for the target strand in dsDNA clearly shifted the equilibrium toward the invasion or strand displaced state, and then the population of the pMB/dsDNA complex was increased. As shown in Figure 4d, the fluorescence enhancement occurred only in the case of dsDNA (G/C), suggesting that the allele specific detection in dsDNA was achieved by our photo-cross-linking strategy using pMB. In the case of using ctl-MB, which did not have photoreactive ^{CNV}K moiety, no fluorescence enhancement occurred. This result also indicates that the fluorescence enhancement was caused by the photo-cross-linking induced equilibrium shift toward a pMB/dsDNA-complexed state. A small decrease in the fluorescence intensity was observed in the case of all dsDNA without dsDNA (G/C), suggesting that the photoirradiation caused the photobleaching of Cy3 at the 5′ termini of the pMB. Fluorescence imaging of the mixture of pMB and dsD-NA before and after the photoirradiation was performed by an excitation with the 520 nm LED lamp (Figure 4e). In the case of dsDNA (G/C), bright fluorescence was observed after the photoirradiation, although the fluorescence was scarcely observed in the other cases, indicating that the pMB has the potential for SNPs typing based on a fluorescence imaging system. Two possible complexes between pMB and target DNA were proposed, i.e., strand invasion or replaced complex. To confirm this, fluorescence spectroscopic analysis using unlabeled pMB, 5′ Cy3-labeled target strand in dsDNA (G/C) and its complementary strand labeled with Dabcyl at the 3′ termini, was performed (Figure S10, Supporting Information). After photoirradiation under the same conditions as those shown in Figure 4c, no fluorescence enhancement was observed, indicating that the end of the target double strand still hybridized after the photo-cross-linking reaction between unlabeled pMB and Cy3 labeled target strand. This strongly suggests that the invasion complex between pMBs and target dsDNAs is a major species of photo-cross-linked complexes under the presented conditions.

Genotyping of Japanese Rice Strains by Photoreactive Molecular Beacons. Four strains of Japanese rice,

dx.doi.org/10.1021/ja406965f | J. Am. Chem. Soc. 2013, 135, 16161−16167

	Sequence 5′–3′*
pMB-1	Cy3-ACATTCAGAGGTCGCATAXTCATAGGAATGT-Dabcyl
pMB-2	Cy3-ACATTCCGAGGGCCCAAXTGGCAAGAAATGT-Dabcyl
pMB-3	Cy3-ACATTCATGCTACACCTCTAXCATGGAATGT-Dabcyl
pMB-1*	Cy3-ACATTCAGAGGTCGCGTAXTCATAGGAATGT-Dabcyl
pMB-2*	Cy3-ACATTCCGAGGGCCCCAXTGGCAAGAAATGT-Dabcyl
pMB-3*	Cy3-ACATTCATGCTACACGTCTAXCATGGAATGT-Dabcyl
dsDNA-1**,†	TATATATTCGACTATGACTAYGCGACCTCTAGTGGTACAC
dsDNA-2**,††	CACCACAGTGGCTTGCCACTYGGGCCCTCGCGTGTCGCCC
dsDNA-3**,†††	GCCGGCCTCGTCATGATAGAYGTGTAGCATATGAGTTATA

*X, under bar, and bold character indicates ^{CNV}K, SNP site, and photocrosslinking site, respectively. **Only the target strands were shown here. Equimolar mixture with their complementary olgonucleotides were annealed and used as dsDNAs. †Y represents T (in the case of AH) or C (in the case of NB, SS and KH). ††Y represents T (in the case of NB) or G (in the case of AH, SS and KH). †††Y represents G (in the case of SS) or C (in the case of NB, AH and KH).

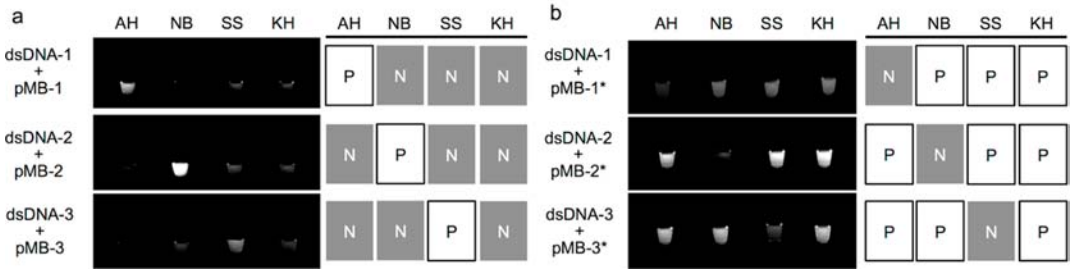

Figure 5. SNP-based genotyping of Japanese rice strains using pMB by fluorescence imaging. (a) Positive detection using pMB-1, -2, and -3. (b) Negative detection using pMB-1*, -2*, and -3*. The table of the predicted results shows the sides of each fluorescence image. "P" and "N" indicate "positive" and "negative" detection, respectively.

Akihikari (AH), Nipponbare (NB), Senshou (SS), and Koshihikari (KH), were adopted to demonstrate the SNPs-based genotyping using pMBs. For the positive detection and the negative detection of the specific SNPs, pMBs having a complementary sequence for one of these four strains (pMB-1, -2, and -3) and three of these four strains (pMB-1*, -2*, and -3*) were designed, respectively. Double-stranded DNAs (dsDNAs) containing three SNP sites of these rice strains were added to the pMBs, UV irradiated, and then the fluorescence image was obtained on a fluorescence imaging system (Figure 5). In the case of the positive detection of strain specific SNP on dsDNA-1 (Figure 5a, top), bright fluorescence was observed only when the dsDNA-1 having AH typed SNP (T/A allele) was added, indicating that the AH typed SNP on dsDNA-1 was clearly detected by using pMB.

In the case of the other SNP sites, dsDNA-2 and -3, the brightest fluorescence was observed only when NB or SS typed dsDNAs were added. The results coincide with the predicted results, suggesting that rice strains would identify with the pattern of the fluorescence image from the positive detection of specific SNPs on dsDNA. In the case of the negative detection of strain specific SNP on dsDNA-1 (Figure 5b, top), weak fluorescence was observed only when the dsDNA-1 having AH typed SNP (T/A allele) was added, indicating that the AH typed SNP on dsDNA-1 was negatively detected by using pMB-1*. In the case of the other SNP sites, dsDNA-2 and -3, weak fluorescence was observed only when NB or SS typed dsDNA were added. The results coincide with the predicted results, suggesting that rice strains would also identify with the pattern of the fluorescence image from the negative detection of specific SNPs on dsDNA. As these two approaches, i.e., positive and negative SNPs identification, were both available for the identification of rice strains, the combination of these approaches would enable more accurate genotyping of Japanese rice strains using pMBs.

CONCLUSION

From the kinetic, thermodynamic, and NMR structural analysis of the photoproduct, we successfully demonstrated that the ^{CNV}K photo-cross-linked to a thymine base in the complementary DNA strand through the *trans* isomer of cyanovinyl moiety and the cyclobutane formation process is a rate-determining step of the photo-cross-linking reaction. These results suggest that the *cis*–*trans* isomer does not largely affect the efficiency of the photo-cross-linking reaction. Using the ultrafast photo-cross-linking reaction, the strand invasion of MB to dsDNA was accelerated and the MB-based SNPs typing of Japanese rice strains using the dsDNA target was achieved.

ASSOCIATED CONTENT

Supporting Information

List of oligonucleotide sequences and MALDI-TOF-MS data; NMR spectra of the *trans* isomer of ^{CNV}K; HPLC chromatograms of ^{CNV}K photoisomerization in ssDNA and dsDNA; UPLC chromatograms of photo-cross-linking reaction of ODN(AX) and cODN(TT); UV melting curves; SPR sensorgrams; NOESY, COSY, HMBC, and HSQC spectra of the photodimer consisting of ^{CNV}K and T; PAGE analysis of the photo-cross-linking reaction of pMBs. This material is available free of charge via the Internet at http://pubs.acs.org.

AUTHOR INFORMATION

Corresponding Author

kenzo@jaist.ac.jp

Notes

The authors declare no competing financial interest.

ACKNOWLEDGMENTS

This study was partly supported by the Grant-in-Aid for Scientific Research (B), Scientific Research (S) and Scientific Research on Innovative Areas (Molecular Robotics) (90293894, K.F.) of The Ministry of Education, Science, Sports and Culture of Japan.

REFERENCES

(1) Lee, B. L.; Murakami, A.; Blake, K. R.; Lin, S. B.; Miller, P. S. *Biochemistry* **1988**, *27*, 3197−3203.
(2) Pieles, U.; Englisch, U. *Nucleic Acids Res.* **1989**, *17*, 285−299.
(3) Teare, J.; Wollenzien, P. *Nucleic Acids Res.* **1989**, *17*, 3359−3372.
(4) Kean, J. M.; Murakami, A.; Blake, K. R.; Cushman, C. D.; Miller, P. S. *Biochemistry* **1988**, *27*, 9113−9121.
(5) Millera, P. S.; Bhana, P.; Cushmana, C. D.; Keana, J. M.; Levisa, J. T. *Nucleosides Nucleotides* **1991**, *10*, 37−46.
(6) Higuchi, M.; Kobori, A.; Yamayoshi, A.; Murakami, A. *Bioorg. Med. Chem.* **2009**, *17*, 475−483.
(7) Higuchi, M.; Yamayoshi, A.; Yamaguchi, T.; Iwase, R.; Yamaoka, T.; Kobori, A.; Murakami, A. *Nucleosides Nucleotides. Nucleic Acids* **2007**, *26*, 277−290.
(8) Murakami, A.; Yamayoshi, A.; Iwase, R.; Nishida, J.; Yamaoka, T.; Wake, N. *Eur. J. Pharmac. Sci.* **2001**, *13*, 25−34.
(9) Giovannangeli, C.; Diviacco, S.; Labrousse, V.; Gryaznov, S.; Charneau, P.; Helene, C. *Proc. Natl. Acad. Sci. U.S.A.* **1997**, *94*, 79−84.
(10) Liu, J.; Geng, Y.; Pound, E.; Gyawali, S.; Ashton, J. R.; Hickey, J.; Woolley, A. T.; Harb, J. N. *ACS Nano* **2011**, *5*, 2240−2247.
(11) Yoshimura, Y.; Fujimoto, K. *Org. Lett.* **2008**, *10*, 3227−3230.
(12) Fujimoto, K.; Konishi-Hiratsuka, K.; Sakamoto, T.; Yoshimura, Y. *ChemBioChem* **2010**, *11*, 1661−664.
(13) Fujimoto, K.; Konishi-Hiratsuka, K.; Sakamoto, T. *Int. J. Mol. Sci.* **2013**, *14*, 5765−5774.
(14) Fujimoto, K.; Yoshinaga, H.; Yoshio, Y.; Sakamoto, T. *Org. Biomol. Chem.* **2013**, *11*, 5065−5068.
(15) Yoshimura, Y.; Ohtake, T.; Okada, H.; Fujimoto, K. *ChemBioChem* **2009**, *10*, 1473−1476.
(16) Fujimoto, K.; Konishi-Hiratsuka, K.; Sakamoto, T.; Yoshimura, Y. *Chem. Commun.* **2010**, *46*, 7545−7547.
(17) Fujimoto, K.; Kishi, S.; Sakamoto, T. *Photochem. Photobiol.* **2013**, DOI: 10.1111/php.12118.
(18) Shigeno, A.; Sakamoto, T.; Yoshimura, Y.; Fujimoto, K. *Org. Biomol. Chem.* **2012**, *10*, 7820−7825.
(19) Tagawa, M.; Shohda, K.; Fujimoto, K.; Suyama, A. *Soft Matter* **2011**, *7*, 10931−10934.
(20) Gerrard, S. R.; Hardiman, C.; Shelbourne, M.; Nandhakumar, I.; Nordén, B.; Brown, T. *ACS Nano* **2012**, *6*, 9221−9228.
(21) Fujimoto, K.; Konishi-Hiratsuka, K.; Sakamoto, T.; Ohtake, T.; Shinohara, K.; Yoshimura, Y. *Mol. BioSyst.* **2012**, *8*, 491−494.
(22) Koning, T. M. G.; van Soest, J. J. G.; Kaptein, R. *Eur. J. Biochem.* **1991**, *195*, 29−40.
(23) Kao, J. L.-F.; Nadji, S.; Taylor, J.-S. *Chem. Res. Toxicol.* **1993**, *6*, 561−567.
(24) Sokol, D. L.; Zhang, X.; Lu, P.; Gewirtz, A. M. *Proc. Natl. Acad. Sci. U.S.A.* **1998**, *95*, 11538−11543.
(25) Nitin, N.; Bao, G. *Bioconjugate Chem.* **2008**, *19*, 2205−2211.
(26) Jayagopal, A.; Halfpenny, K. C.; Perez, J. W.; Wright, D. W. *J. Am. Chem. Soc.* **2010**, *132*, 9789−9796.
(27) He, Y.; Zeng, K.; Gurung, A. S.; Baloda, M.; Xu, H.; Zhang, X.; Liu, G. *Anal. Chem.* **2010**, *82*, 7169−7177.
(28) Lin, Y.-W.; Ho, H.-T.; Huang, C.-C.; Chang, H.-T. *Nucleic Acids Res.* **2008**, *36*, e123.
(29) Gerasimova, Y. V.; Hayson, A.; Ballantyne, J.; Kolpash-chikov, D. M. *ChemBioChem* **2010**, *11*, 1762−1768.
(30) Farjami, E.; Clima, L.; Gothelf, K.; Ferapontova, E. E. *Anal. Chem.* **2011**, *83*, 1594−1602.
(31) Ortiz, E.; Estrada, G.; Lizardi, P. M. *Mol. Cell. Probes* **1998**, *12*, 219−226.
(32) Kuhn, H.; Demidov, V. V.; Coull, J. M.; Fiandaca, M. J.; Gildea, B. D.; Frank-Kamenetskii, M. D. *J. Am. Chem. Soc.* **2002**, *124*, 1097−1103.
(33) Nielsen, P. E.; Egholm, M. *Current Issues Molec. Biol.* **1999**, *1*, 89−104.